# A novel route for the controlable synthesis of magnetite nanoparticles

P. Tserotas

**Abstract**— Nanoparticles of magnetite ($Fe_3O_4$) were obtained via a novel synthetic route. First, iron enneacarbonyl, $Fe_2(CO)_9$, was prepared by the decomposition reaction of liquid iron pentacarbonyl, $Fe(CO)_5$, injected in a hexane solvent in the presence of sunlight and mild heating. In the second step, the resulting dry $Fe_2(CO)_9$ crystals were complexed with β-Cyclodextrin (β-CD) molecules, leading to steric hindrance of the organometallic crystals among the interstices of the CD molecular network; the latter mediates both particle size control and protection of the nanoparticles from further oxidation and agglomeration. The β-CD organometallic complex system, obtained in the previous step, was thermally treated, initiating a polyol process, in the presence of high boiling-point 1, 12 dodecanediol which acted both as a reductant and a solvent. Following a final addition of oleic acid, the solution was then refluxed, forming magnetite nanoparticles. The obtained particles were characterized by X-ray diffraction which showed a face-centered cubic spinel structure with diffraction peaks of magnetite. Fourier Transform Infrared spectroscopy revealed the existence of magnetite coated with hydrophobic oleic acid, as well as the existence of hydrophilic unitsand. Highresolution transmission electron microscopy indicated that the nanoparticles were isolated, nearly monodispersed and almost spherical.

**Index Terms**— Magnetic nanoparticles, magnetite, maghemite, cyclodextrin, organometallics.

———————————— ◆ ————————————

## 1 INTRODUCTION

Several processing routes that follow the off-equilibrium state [1], [2], [3], [4], [5], [6], [7], [8] often lead to functional materials such as light alloys with extended solid solubility [9], [10], [11], [12], [13], [14], [15], [16] and amorphous alloys with superb corrosion properties [17], [18], [19], [20], [21], [22]. Regarding the hydrometallurgy routes, these, in recent years, have yielded magnetic nanoparticle materials, with unprecedented properties, comparing with their bulk counterparts. For example, magnetite nanoparticles are of great interest within the realms of magnetic fluids [23], catalysis [24], [25], biotechnology [26], magnetic resonance imaging [27], data storage [28] and environmental remediation [29]. Successful applications demand the particles, to be chemically stable under a range of various conditions. The nanoparticles that are normally used are below a critical size, which is dependent on the application, and is typically 10 to 20 nm. Within this range, each nanoparticle acts as a single magnetic domain and shows superparamagnetic behaviour when the temperature is above the so-called blocking temperature [30].

A variety of techniques have been developed for the efficient production of nanoparticles, including metal evaporation [31], thermal decomposition, coprecipitation and chemical reduction methods [32], as well as laser pyrolysis [33]. Thermal decomposition, in particular, is one of the widely used chemical approaches for the production of nanoparticles. In this method, the nuclei are formed after precursors are added to a solution in the presence of surfactants at sufficiently high temperatures, such that the precursors may be decomposed. In this method, particle properties depend on the reaction parameters, including reaction time, temperature and the type of surfactants used. Among the various precursors utilised, iron pentacarbonyl, $Fe(CO)_5$, is of increased merit. Also referred to as iron carbonyl, iron pentacarbonyl is the main precursor in the synthesis of magnetite ($Fe_3O_4$) or maghemite (γ-$Fe_2O_3$) via thermal decomposition. Indicatively, Park et al synthesized monodisperse γ-$Fe_2O_3$ nanoparticles with average diameters in the range of 4 to 16 nm using a $Fe(CO)_5$ precursor and oleic acid surfactant [34].

Iron pentacarbonyl is also metastable, with a formation enthalpy of -185 kcal/mol and a formation enthalpy of each of the five carbon monoxide subunits equal to -110.5 kcal/mol, which account for the compound's tendency to decompose via a complicated reaction pathway; the latter may also involve a range of intermediate iron carbonyls. Numerous surfactants and other species can also catalyse this decomposition reaction and, as a result, the reaction frequently changes rate and even order, which is always a crucial factor when attempting to grow nanoparticles of controlled size and shape [35]. There exist numerous reports in the literature for inclusion complexation of organometallic compounds with cyclodextrin molecules, with the latter acting both as host molecules and as mediators for various organic oxidation and catalytic reactions [36], [37], [38], [39], [40], [41].

The current work presents a synthesis route which is aimed at the synthesis of monodispersed magnetite nanoparticles. The route has been designed to take advantage of the facile decomposition of unstable $Fe(CO)_5$, which is converted in a hexane solution to stable iron enneacarbonyl, $Fe_2(CO)_9$, in the form of crystals, under specific conditions [42]. Next, this organometallic compound is complexed with β-Cyclodextrin molecules, according to a combination of two modified complexation procedures described elsewhere [43].

———————————————

• *Philippos Tserotas posess a master degree in chemical engineering from the National Technical University of Athens, Greeece. As a research associate, he collaborates with research teams under various projects. E-mail: phit-ser@gmail.com*

It is noteworthy that iron enneacarbonyl was utilised both as a guest compound for complexation with cyclodextrin molecules and as an iron precursor for the synthesis of magnetic nanoparticles.

## 2  MATERIALS AND METHODS

The cyclodextrin molecular network seems to constitute an ideal platform for the synthesis of nanoparticles of narrow size distribution and monodispersity.

Cyclodextrins [44], [45], [46], [47], [48], [49], [50] are cyclic oligosaccharides composed of α-(1, 4) linked glucopyranose subunits, with an extreme inclusion complex capability, due to their cage-like supramolecular structure. The cyclodextrin cavity is hydrophobic, while the external surface is hydrophilic due to the existence of hydroxyl groups. Two different faces may be distinguished on CDs. The narrow cavity side has primary hydroxyl groups and is called the primary face. The large cavity side bears secondary hydroxyl groups and is called the secondary phase. By taking advantage of the cyclodextrin capability to form inclusion complexes with a variety of compounds, including organometallics, it was managed to obtain such a complex system with β-CD. The cyclodextrin molecular network acts both as a size controller, an adsorbent platform and a stabilizing factor, by sterically hindering the organometallic molecules among the interstices/cavities of the CD molecules. The prepared system was subjected to a polyol process, inclusive of a mild thermal treatment, in the presence of a high boiling point alcohol, 1, 12 dodecanediol, both as a reductant and a solvent. Finally, after the addition of oleic acid, the system was refluxed and the monodispersed magnetite nanoparticles were thus obtained.

### 2.1 Chemicals

The chemicals used were β-Cyclodextrin (β-CD), iron pentacarbonyl, $Fe(CO)_5$, 1,12 dodecanediol, oleic acid (OA), acetone (Ac), ethanol (EtOH); they were all purchased from Alfa Aesar and they were not submitted to further purification. The chemical synthesis was carried out in a glove box.

### 2.2 The iron enneacarbonyl organometallic complex formation

Iron enneacarbonyl, a stable organometallic compound, $Fe_2(CO)_9$, was obtained by an iron pentacarbonyl metastable organometallic complex, $Fe(CO)_5$. A quantity of 5 ml of $Fe(CO)_5$ were injected to a 100 ml flask, containing 40 ml of a hexane solution. The flask was then sealed and was heated to 50-60 °C for 2 h. This mild thermal treatment initiated the decomposition of iron pentacarbonyl and the formation of the first $Fe_2(CO)_9$ crystals, that were visible at the bottom of the flask. After that step of initial thermal treatment, the flask was left exposed to sunlight for 3 days, until the decomposition reaction of $Fe(CO)_5$ was complete. In total, totally 0.52 g (1.4 mmol) of air stable crystals of iron enneacarbonyl was obtained via gradual hexane evaporation.

### 2.3 The complexed precursor preparation

The preparation of the complex system between βCyclodextrin and $Fe_2(CO)_9$ crystals was carried out according to a combination of two modified complexation procedures. The molar ratio of the organometallic complex compound, $Fe_2(CO)_9$ to the β-CD was set to 4:1. The as-prepared dry crystals of the organometallic compound were then dispersed in a 10 ml acetone solution (solution A). In a parallel step, 0.40 g of β-CD (0.35 mmol) was dissolved under vigorous stirring, in a 100 ml flask containing 32 ml of distilled water, until the solution became almost saturated (solution B). Then, again under vigorous stirring and mild heating (55-60 °C), solutions A and B were mixed. After 30 minutes, the colour of the solution turned to dark brown. The temperature was then gradually increased to 80-100 °C and the stirring procedure was continued until the solution finally dried. The obtained product precipitated at the bottom of the flask in the form of an organometallic system complexed with β-CD (powder), with a dark-brown colour and a weight of 0.80 g. This was utilized as a precursor for the next synthetic step which was the formation of magnetite nanoparticles.

### 2.4 The magnetite nanoparticles synthetic route

This particular multi-step synthetic route was carried out as follows: In the first step, 0.4 g of the complexed precursor with β-CD were dispersed under stirring for 20 minutes, in a flask containing a mixture of distilled $H_2O$/EtOH, at a molar ratio 4:1; this step aimed at removing impurities as well as any remaining noncomplexed β-CD from the previous complexation procedure. In the second step, the remaining pure complexed system was obtained by filtration and was then dried. Then, it was added to a three-neck round-bottom flask, along with 2 g of 1, 12 dodecanediol, and was then heated to 100 °C in ambient conditions under stirring for 30 minutes. Finally, 1.5 ml of oleic acid was added to the previous solution which was submitted to refluxing for 1 hour. Gradually, the colour of the solution turned to black. After the refluxing procedure, the system was cooled to room temperature and the synthesized nanoparticles were flocculated and precipitated via the addition of ethanol. Then, the magnetic nanoparticles were collected from the flask, with the aid of a powerful permanent magnet and washed several times with ethanol solution. Finally, the obtained magnetic material was redispersed in a hexane solution.

### 2.5  Particles characterization

The produced nanopowders were analyzed by X-ray diffraction (XRD), using a Bruker D8-Focus diffractometer with nickel-filtered Cu-Kα radiation (=1.5405 Å), operating at 40 kV and 40 mA. Transmission Electron Microscopy (TEM) studies were performed on a Jeol 2100 HR microscope; TEM samples were prepared by forming a suspension of the particles with a concentration of between 0.1 and 0.01 wt% solid fraction. Finally, powders were characterized by a Perkin Elmer Spectrum GX Fourier Transform IR spectrophotometer, in the range of 4000–400 cm−1 with 200 successive scans. The spectrometer was equipped with a deuterated triglycine sulphate (DTGS) detector and with an attenuated total reflectance (ATR) unit.

## 3 RESULTS AND DISCUSSION

In the current study, monodispersed magnetite nanoparticles

were synthesized via a combination of polyol and thermal decomposition process. The utilized iron source, the organometallic precursor compound, $Fe_2(CO)_9$, was obtained and complexed with β-CD. Under a three step synthetic route, including rinsing/purification, mild thermal treatment-polyol process, in the presence of 1, 12 dodecanediol and refluxing in the presence of oleic acid, this complexation product formed the magnetic material.

## 3.1 Stractural Characterization

The XRD profile of the synthesized magnetic nanoparticles is illustrated in fig1. As it can be seen, characteristic peaks are visible (220, 311, 400, 422, 511, 440 at 2θ~300, 350, 430, 530, 570, 630 respectively), which are indicative of a face-centered cubic spinel structure with diffraction peaks of magnetite, according to the JCPDS card no. 019-0629. This indicates that the synthesized nanoparticles are Fe3O4. Large particles diameters (> 8nm), as is the current case, favor the Fe3O4 structure. This is attributed to the balance between the Fe oxidation states; the higher the oxidation state is, the higher the specific surface area becomes.
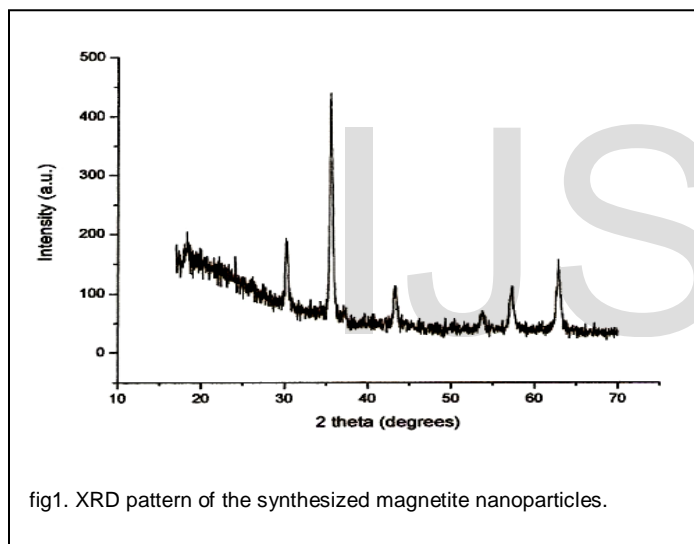


fig1. XRD pattern of the synthesized magnetite nanoparticles.

The FT-IR spectrum of synthesized nanoparticles is illustrated in fig2. Characteristic peaks at 3440 cm-1 (β-CD group), 2923-2853 cm-1(hydroxyl groups due to β-CD complexation), 1711-1631 cm-1(carbonyl groups)and 555 cm-1(ferrite peak) confirm the existence of magnetite coated with hydrophobic oleic acid, as well as the existence of hydrophilic units.

The OA magnetic nanoparticles of the present study in a low and high TEM resolution are depicted in fig3a and fig3b, respectively. The nanoparticles were isolated, nearly monodispersed, and were almost spherical. The oleic acid molecules appeared to keep the particles isolated from each other reducing interactions. The average core particle size and standard deviation obtained from 200 particles using the Image-Pro Plus analytic suite was 9.6 ± 0.8 nm. (a) The magnetic nanoparticles that were synthesized in smaller resolution, (b) The magnetic nanoparticles that were synthesized in larger resolu-

tion, (c) a large resolution of a TEM micrograph where the (311) lattice fringes are noticeable.
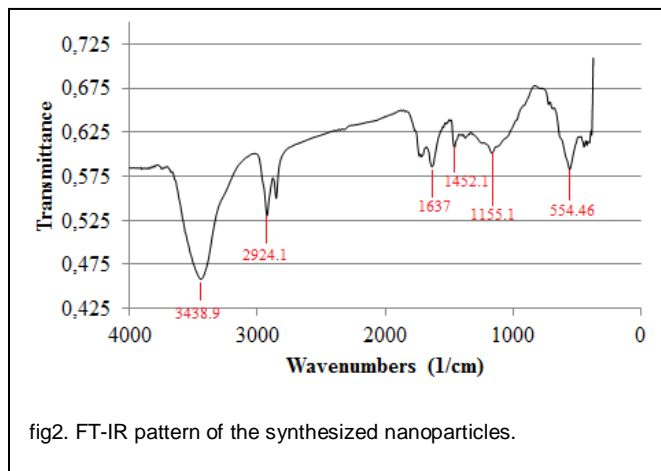


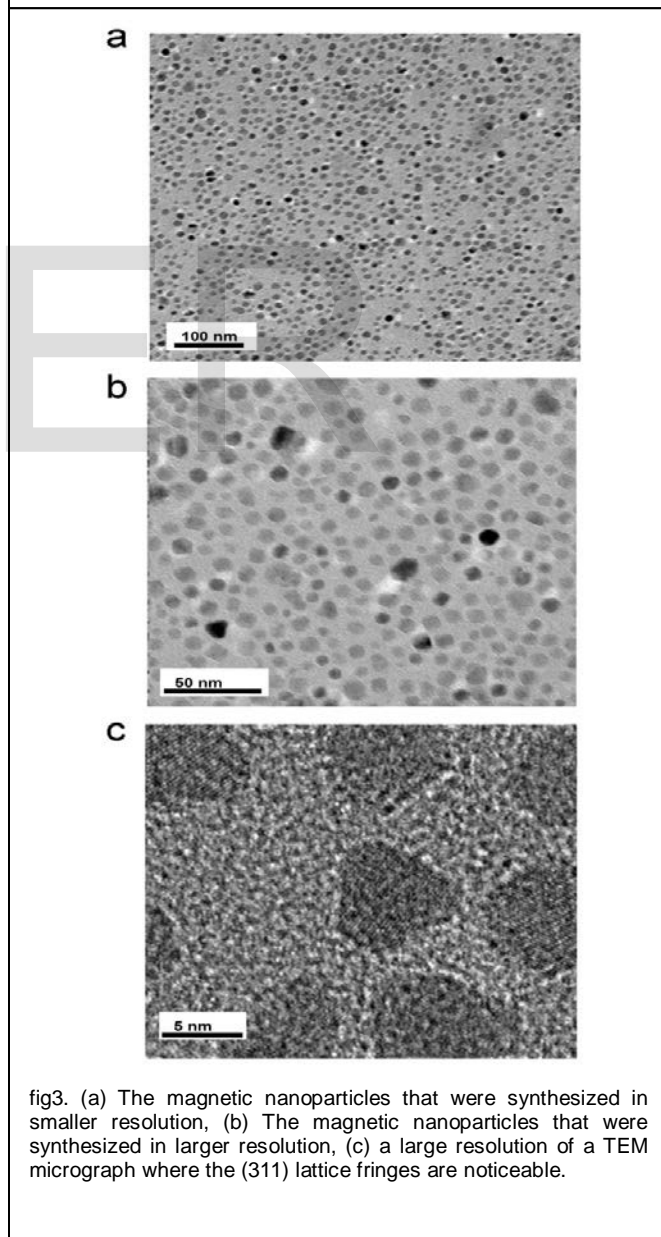fig2. FT-IR pattern of the synthesized nanoparticles.



fig3. (a) The magnetic nanoparticles that were synthesized in smaller resolution, (b) The magnetic nanoparticles that were synthesized in larger resolution, (c) a large resolution of a TEM micrograph where the (311) lattice fringes are noticeable.

## 3.2 The role of 1, 12 dodecanediol in conjunction with β-Cyclodextrin during the polyol process

During the polyol process, 1, 12 dodecanediol was utilized both as a reductant and a solvent for the complex system βCD/Fe$_2$(CO)$_9$. Both the latter and β-Cyclodextrin posess the same functional group (–OH), with 1, 12 dodecanediol bearing two primary hydroxyl groups in its molecule and β-CD having two network structures of primary and secondary (–OH) group. The presence of this common functional group suggests that these compounds behave similarly and have a similar functionality.

In the step of mild thermal treatment at 100 ∘C, the hydroxyl groups of both compounds appear to play a central role in the homogenization of the mixture and the redox phenomena which are associated to the polyol process. At 100 ∘C in ambient conditions, during the melting of dodecanediol, water molecules are released in the reaction vessel, due to the initiation of its oxidation to aldehydes and ketones. The existing βcyclodextrin also participates in the oxidation procedure. It is believed that, from the complexation procedure, β-CD molecules have, mainly, physically adsorbed via Van der Waals forces, on the hydrophobic crystals of Fe$_2$(CO)$_9$, rendering them somewhat hydrated or hydrophilic with their hydroxyl groups network. This facilitated their mixing with dodecanediol. Of course, the (– OH) groups of CD molecules are also oxidized with further heating. Both 1, 12 dodecanediol and βcyclodextrin are considered to belong to a category of polyol compounds and, depending on the experimental conditions (in the current work: first heating at 100 ∘C in open air and then refluxing at 300 ∘C), their hydroxyl functional groups are oxidized to aldehydes, carboxylic acids, or intermediate compounds with joint functions.

At the same time, according to the literature, iron enneacarbonyl crystals start decomposing at 80 ∘C:

$$2Fe_2(CO)_9 \rightarrow 2Fe(CO)_5 + 2Fe(CO)_4 \qquad (1)$$
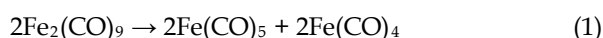
By further heating a parallel reaction takes place:

$$2Fe(CO)_4 \rightarrow Fe(CO)_5 + Fe + 3CO \qquad (2)$$
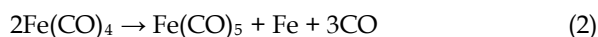
Undoubtedly, the decomposition does not always follow a simple pathway and a range of intermediate iron carbonyls and iron clusters can form and may catalyze the decomposition of (1). It is, therefore, anticipated that at 100 ∘C, various intermediate iron carbonyls/clusters have formed within the β-CD network. These have most likely interacted with β-CD and dodecanediol oxidation products (aldeydes/carboxylic acids), mainly at higher temperatures within the refluxing step.

## 3.3 The role of oleic acid during the thermal decomposition process -The local controlled oxidation mechanism provided by β-CD network

Herein, the aforementioned obtained complex system is refluxed at 300 ∘C in the presence of oleic acid. The role of the organic acid is of paramount importance as it strongly interacts with the intermediate iron carbonyls formed in the β-CD network. From this interaction, iron oleate complexes are formed, according to a general scheme reaction:

$$Fe(CO)x + OA \rightarrow Fe(oleate)x + XCO \qquad (3)$$
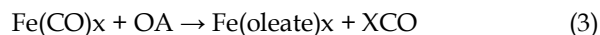
These complexes are the final iron precursors which eventually decompose to yield the magnetite nanoparticles at the specific refluxing temperature range. There is a general consensus that various surfactants, such as oleic acid, play a catalytic role in the decomposition of metal carbonyls. The same has been concluded for some polymeric compounds. In the case of iron enneacarbonyl, Fe$_2$(CO)$_9$, in the current study, oleic acid appears to accelerate the decomposition of the organometallic compound according to the general scheme of (3), providing a fast nucleation process to the reaction system, prior to the slower process of particle growth. Furthermore, oleic acid acts as a stabilizing and oxidation-protective agent-surfactant for the synthesized nanoparticles. At this point, it is noted that the initial complex precursor compound, i.e. the adsorbed β-CD molecules, provides effective steric hindrance to the newly formed nanoparticles.

This leads to size-selective precipitation of the generated nanoparticles by the end of the refluxing procedure, together with the addition of ethanol. Another, important issue is that of the effectively controlled oxidation mechanism on the surface of the formed nuclei-iron nanoclusters, which seems to take place prior to or in conjunction with the growth stage. This decisively determines the magnetite structure of the final nanoparticles. There are strong indications that, under the increased temperature of the refluxing procedure, the dense hydroxyl network of CD molecules, being adsorbed onto the precursor organometallic complex molecules either partially or totally, is transformed to a local oxidative molecular network of carboxylic and aldehydic groups. This combination of hydroxyl and carboxylic/aldehydic groups provides a well-controlled, local surface oxidation mechanism through the binding of those groups on the generated iron nanoclusters, by mainly forming magnetite (Fe$_3$O$_4$) instead of maghemite (γ-Fe$_2$O$_3$) or hematite (α-Fe$_2$O$_3$) nanoparticles, during the nucleation-growth step. This indication is reinforced by the coexistence of oleic acid and the strong reductive environment provided from dodecanediol and CO released in the reaction system during the decomposition, the latter protecting the newly formed nanoparticle material from full oxidation.

## 4 CONCLUSIONS

The particular multi-step synthetic route accomplished to yield magnetite nanoparticles of a highly controllable size (approximately 10 nm). In the process, at first, a novel organometallic precursor, Fe$_2$(CO)$_9$, was obtained, in order to be utilized as the iron source for further nanoparticle synthesis. Secondly, β-Cyclodextrin molecules were chosen as the best candidates of molecular host compounds, in order to form a complex system with Fe$_2$(CO)$_9$ (guest compound). In turn, β-CD molecules, due to their bulky structure within their hydrophobic cavities/interstices, provided effective steric hindrance to the organometallic molecules. Then, the obtained β-CD organometallic complex system underwent thermal treat-

ment (a polyol process) in the presence of a high boiling point alcohol, 1, 12 dodecanediol, which acted both as a reductant and a solvent. Further, after the addition of oleic acid, the above solution was refluxed, forming the magnetite nanoparticles. The as-synthesized nanoparticles were largely mono-dispersed and of uniform shape.

## ACKNOWLEDGMENT

## 5 REFERENCES

[1] Antipas, G.S.E., Plasma-spray synthesis and characterization of Ti-based nitride and oxide nanogranules. Materials Research (submitted for publication).

[2] Antipas, G.S.E., Surface growth and diffusion energetics of Ag mono-layers on Cu (001). Metals, 2014. 4(2): p. 108-117.

[3] Antipas, G.S.E., Augmentation of wearprotective coatings for non-ferrous alloys by the addition of Cr and Ni elements. Materials Research, 2014.

[4] Antipas, G.S.E., A mass efficiency test of α-β processed Ti-Al-V alloys. Key Engineering Materials, 2014. 605: p. 605-608.

[5] Antipas, G.S.E., The Effect of Increasing Sn Content on High-Temperature Mechanical Deformation of an Mg-3%Cu-1%Ca Alloy. Metals, 2013. 3: p. 337-342.

[6] Antipas, G.S.E., A review of gas atomization and spray forming phenomenology. Powder Metallurgy, 2013.

[7] Antipas, G.S.E., Spray forming of al alloys: Experiment and theory. Materials Research, 2012. 15(1): p. 131-135.

[8] Antipas, G., Gas Atomization of Aluminium Melts: Comparison of Analytical Models. Metals, 2012. 2(2): p. 202-210.

[9] Antipas, G.S.E., C. Lekakou, and P. Tsakiropoulos, Microstructural characterization of Al—Hf and Al—Li—Hf spray deposits. Materials Characterization, 2011. 62(4): p. 402-408.

[10] Antipas, G.S.E., Liquid column deformation and particle size distribution in gas atomisation. International Journal of Computational Materials Science and Surface Engineering, 2011. 4(3): p. 247-264.

[11] Antipas, G.S.E., Modelling of the break up mechanism in gas atomization of liquid metals Part II. The gas flow model. Computational Materials Science, 2009. 46(4): p. 955-959.

[12] Antipas, G.S.E., Modelling of the break up mechanism in gas atomization of liquid metals. Part I: The surface wave formation model. Computational Materials Science, 2006. 35(4): p. 416-422.

[13] Antipas, G., C. Lekakou, and P. Tsakiropoulos, The break up of melt streams by high pressure gases in spray forming. Proceedings of the Second International Conference on Spray Forming, 1993: p. 15-24.

[14] Antipas, G.S.E., A concise methodology for the estimation of elemental concentration effects on mesoscale cohesion of non-ferrous covalent glasses: the case of Se(80-x)Ge(20-x)Inx=0,5,10,15. Data In Brief, 2015. 4: p. 257-265.

[15] Antipas, G.S.E. and K. Karalis, The effect of annealing on the electronic stability of an amorphous Zr70Pd30 alloy. Materials Chemistry and Physics, 2014. 147(3): p. 1092-1098.

[16] Antipas, G.S.E., Short range order and stability of a mechanically alloyed Cr25Nb75 alloy determined by total scattering and first principles. Materials Research, 2014. 17(6): p. 1677-1685.

[17] Antipas, G.S.E., Molecular orbital interactions in glass-forming Zr70Cu30 liquid quasicrystals. Journal of Alloys and Compounds, 2013. 578: p. 565-570.

[18] Antipas, G.S.E., E. Mangiorou, and E. Hristoforou, Solute-solvent interactions and atomic cohesion in GeSe4 and GeSe4In5 metallic glasses. Materials Research Express, 2014. 1(1): p. 015202.

[19] Antipas, G.S.E. and E. Mangiorou, Atomic topology and electronic structure of a meltspun Al92U8 metallic glass. Computational and Theoretical Chemistry, 2014. 1036: p. 16-21.

[20] A.P. Khandhar, R.M. Ferguson, J.A. Simon, K.M. Krishnan., Tailored magnetic nanoparticles for optimizing magnetic fluid hyperthermia. Journal of Biomedical Materials Research - Part A, 2012. 100 A(3): p. 728-737.

[21] Lu, A.H., et al., Nanoengineering of a magnetically separable hydrogenation catalyst. Angewandte Chemie - International Edition, 2004. 43(33): p. 4303-4306.

[22] Tsang S.C., Caps V., Paraskevas I., Chadwick D., Thompsett D., Magnetically separable, carbon-supported nanocatalysts for the manufacture of fine chemicals. Angewandte Chemie - International Edition, 2004. 43(42): p. 5645-5649.

[23] Gupta, A.K. and M. Gupta, Synthesis and surface engineering of iron oxide nanoparticles for biomedical applications. Biomaterials, 2005. 26(18): p. 3995-4021.

[24] S. Mornet, S. Vasseur, F. Grasset, P. Veverka, G. Goglio, A. Demourgues, J. Portier, E. Pollert, E. Duguet., Magnetic nanoparticle design for medical applications. Progress in Solid State Chemistry, 2006. 34(2-4): p. 237-247.

[25] Hyeon, T., Chemical synthesis of magnetic nanoparticles. Chemical Communications, 2003. 9(8): p. 927-934.

[26] M.Takafuji, S.Ide, H.Ihara, and Z.Xu, Preparation of poly(1-vinylimidazole)-grafted magnetic nanoparticles and their application for removal of metal ions. Chemistry of Materials, 2004. 16(10): p. 1977-1983.

[27] P.Pulišová, J.Kováč, A.Voigt, P.Raschman., Structure and magnetic properties of Co and Ni nano-ferrites prepared by a two step direct microemulsions synthesis. Journal of Magnetism and Magnetic Materials, 2013. 341: p. 93-99.

[28] S. Cingarapu, Z. Yang, C.M. Sorensen, and K.J. Klabunde, Synthesis of indium nanoparticles: Digestive ripening under mild conditions. Inorganic Chemistry, 2011. 50(11): p. 5000-5005.

[29] Antipas G.S.E., Statharas E., Tserotas P., Papadopoulos N., Hristoforou E., Experimental and firstprinciples characterization of functionalized magnetic nanoparticles. ChemPhysChem, 2013. 14(9): p. 1934-1942.

[30] R. Alexandrescu, I. Morjan, I. Voicu, F. Dumitrache, L. Albu, I. Soare, G. Prodan, Combining resonant/non-resonant processes: Nanometerscale iron-based material preparation via CO2 laser pyrolysis. Applied Surface Science, 2005. 248(1-4): p. 138-146.

[31] Park J., Lee E., Hwang N.M., Kang M., Kim S.C., Hwang Y., Park J.G., Noh H.J., Kim J.Y., Park J.H., Hyeon T., One-nanometer-scale sizecontrolled synthesis of monodisperse magnetic iron oxide nanoparticles. Angewandte Chemie - International Edition, 2005. 44(19): p. 2872-2877.

[32] John Z. Wen, C. Franklin Goldsmith, Robert W. Ashcraft, and William H. Green, Detailed kinetic modeling of iron nanoparticle synthesis from the decomposition of Fe(CO)5. Journal of Physical Chemistry C, 2007. 111(15): p. 5677-5688.

[33] Braga S. S., Gago S., Seixas J. D., Valente A.A., Pillinger M., Santos T.M., Goncalves I.S., Romao C.C., β-Cyclodextrin and permethylated β-cyclodextrin inclusion compounds of a cyclopentadienyl molybdenum tricarbonyl complex and their use as cyclooctene epoxidation catalyst precursors. Inorganica Chimica Acta, 2006. 359(15): p. 4757-4764.

[34] Viliam Kolivoška, Miroslav Gál, Magdálena Hromadová, Michal Valášek, Lubomír Pospíšil, Correlation of the formation constant of ferrocene-

cyclodextrin complexes with dielectric properties of the aqueous DMSO solution. Journal of Organometallic Chemistry, 2011. 696(7): p. 1404-1408.

[35] C. Martínez-Boubeta, K. Simeonidis, M. Angelakeris, N. Pazos-Pérez, M. Giersig, A. Delimitis, L. Nalbandian, V. Alexandrakis, and D. Niarchos, Critical radius for exchange bias in naturally oxidized Fe nanoparticles. Physical Review B - Condensed Matter and Materials Physics, 2006. 74(5).

[36] S. S. Braga, S. S. Rodrigues, C. C. L. Pereira, Z. Petrovski, Synthesis of ferrocenyldiimine metal carbonyl complexes and an investigation of the Mo adduct encapsulated in cyclodextrin. New Journal of Chemistry, 2005. 29(2): p. 347-354.

[37] Zhang, W., M. Chen, and G. Diao, Preparation and electrochemical behavior of water-soluble inclusion complex of ferrocene with βcyclodextrin polymer. Electrochimica Acta, 2011. 56(14): p. 5129-5136.

[38] Zhao, W. and Q. Zhong, Recent advance of cyclodextrins as nanoreactors in various organic reactions: A brief overview. Journal of Inclusion Phenomena and Macrocyclic Chemistry, 2012. 72(1-2): p. 1-14.

[39] Huber, D.L., Synthesis, properties, and applications of iron nanoparticles. Small, 2005. 1(5): p. 482-501.

[40] Blanchard, A.A., The volatile metal carbonyls. Chemical Reviews, 1937. 21(1): p. 3-38.

[41] Brewster, M.E. and T. Loftsson, Cyclodextrins as pharmaceutical solubilizers. Advanced Drug Delivery Reviews, 2007. 59(7): p. 645-666.

[42] Del Valle, E.M.M., Cyclodextrins and their uses: a review. Process Biochemistry, 2004. 39(9): p. 1033-1046.

[43] Loftsson, T. and D. Duchêne, Cyclodextrins and their pharmaceutical applications. International Journal of Pharmaceutics, 2007. 329(1-2): p. 1-11.

[44] Nagaraju, M. and G. Narahari Sastry, Theoretical studies on inclusion complexes of cyclodextrins. Journal of Physical Chemistry A, 2009. 113(34): p. 9533-9542.

[45] Schneiderman, E. and A.M. Stalcup, Cyclodextrins: A versatile tool in separation science. Journal of Chromatography B: Biomedical Sciences and Applications, 2000. 745(1): p. 83-102.

[46] Szejtli, J., Past, present, and future of cyclodextrin research. Pure and Applied Chemistry, 2004. 76(10): p. 1825-1845.

[47] Saenger, W., Cyclodextrin Inclusion Compounds in Research and Industry. Angewandte Chemie International Edition in English, 1980. 19(5): p. 344-362.

[48] Saenger, W., Crystal packing patterns of cyclodextrin inclusion complexes. Journal of Inclusion Phenomena, 1984. 2(3-4): p. 445-454.

[49] Tserotas, P., E. Statharas, and I. Kartswnakis, A Novel Synthesis of Monodispersed Magnetite Nanoparticles by an Organometallic Complexed Precursor. Key Engineering Materials, 2014. 605: p. 685-688.

[50] Tserotas, P., E. Statharas, and I. Kartswnakis, A Novel Approach for the Synthesis of PEGylated Monodispersed Superparamagnetic Iron Oxide Nanoparticles. Key Engineering Materials, 2014. 605: p. 693-696.